

# Characterizing the NuLat Detector Employing Coincidence Techniques

Emilio Jarrin<sup>1</sup> and Bruce Vogelaar<sup>2</sup>

<sup>1</sup>*Department of Physics and Astronomy, University of Iowa, Iowa City, IA 52240, USA*

<sup>2</sup>*Center for Neutrino Physics, Virginia Polytechnic Institute and State University, Blacksburg, VA 24060, USA*

(Dated: July 2022)

The Neutrino Lattice Experiment (NuLat) was designed to detect neutrinos, in particular antineutrinos produced from nuclear reactors which may indicate the presence of the so-called “sterile” neutrino. The most recent use of the NuLat detector focuses on the detection of electron antineutrinos via inverse beta decay (IBD). With the use of a scintillating cube lattice that comprises NuLat, signals of positron annihilation and neutron capture that appear from the resulting IBD plus the interactions with the material are collected and amplified by photomultiplier tubes (PMTs) installed in the detector. The objective of this summer’s project was then to characterize the response of NuLat. This was done by employing coincidence techniques that helped overcome background noise. In this case, the gamma spectrum of various radioactive sources was collected with two detectors in coincidence, and the signals generated by the gamma emissions of the sources were used for coincidence triggering. One of the detectors is based on the inorganic scintillator thallium-doped sodium iodide (NaI(Tl)). The other is a single plastic scintillating cube from NuLat which initially will be thoroughly characterized, and this information will be extended to effectively determine a calibration of the NuLat detector.

## I. INTRODUCTION

One of the most active fields of research in particle physics is the study of neutrino oscillation. This is a phenomenon that occurs as the neutrino propagates through space. The neutrino is an elementary particle that belongs to the Standard Model of particle physics. Currently, there are three known types of neutrinos that have a flavor associated to them. The flavors of the neutrino, also called the flavor states, are: the electron neutrino, the muon neutrino, and the tau neutrino. When we try to detect one of the flavored neutrinos, such as the electron neutrinos that are produced in the Sun, only a third of the amount expected appear on Earth. This deficit of neutrino flux can be explained by the theory of neutrino oscillation. The theory states that a flavor state is made of a linear combination of states of definite mass, or mass eigenstates, in which during the propagation of the neutrino the relative phase of the mass eigenstates changes producing the transmutation of the flavors[1]. As a consequence of this effect, we may detect a flavored neutrino that was not originally produced in the source.

Such phenomenon of neutrino oscillation shows that the neutrino has mass and some measurements of these have been recorded although without sufficient precision [3]. This contrasts to the predictions of the Standard Model. According to our current understanding the neutrino should not possess any mass, so the rise of new physics may come along with more studies of neutrino oscillation. Furthermore, recent experiments that emerged from neutrino oscillation suggest there could be another neutrino, a so-called “sterile” neutrino that is distinct to the “active” neutrinos known. Many experiments today seek to find observations of the sterile neutrino, and evidence for this hypothetical particle could provide more information about the nature of the neutrino and its peculiar behavior.

## II. THE NEUTRINO LATTICE EXPERIMENT (NULAT)

The importance of measuring the amounts of neutrino flux is that we can study about neutrino oscillation patterns and search for hints of the sterile neutrino. Some of the ongoing research with such objectives is the Neutrino Lattice Experiment (NuLat) which focuses on the detection of electron antineutrinos that induce Inverse Beta Decay (IBD). The IBD reaction examined with the NuLat detector involves the interaction of an electron antineutrino and a proton, resulting in the emission of a positron and a neutron. This process can be written as

$$\bar{\nu}_e + p \rightarrow e^+ + n . \quad (1)$$

The presence of the antineutrino is determined by the detection of the signals from the corresponding energy depositions of the IBD products, the positron and the neutron. These signals are collected in the NuLat detector and converted into electrical pulses. In the case of the positron, it quickly interacts with matter and annihilates with an electron, producing two prompt back-to-back gamma rays, each with energy of 511 keV. The neutron has a delay time with respect to the positron reflected in the time it takes to slow down and stop. After losing its momentum, the neutron is captured by the lithium that is embedded in the scintillating plastic cubes of NuLat. Here, the cubes are doped with Lithium-6 (<sup>6</sup>Li). When the neutron interacts with <sup>6</sup>Li after its capture, it excites the nucleus to the unstable isotope <sup>7</sup>Li, which then decays emitting an alpha particle and a tritium nucleus (or <sup>3</sup>H), releasing 4.8 MeV of energy.

There are in total 125 scintillating plastic cubes based on polyvinyl toluene (PVT) that compose the interior of NuLat, each doped with <sup>6</sup>Li allowing for neutron capture. The PVT cubes are arranged in a 5 × 5 × 5 lattice such that light generated from the energy deposition is

directed towards photomultiplier tubes (PMTs) through total internal reflection. This arrangement uses the concept of the Raghavan Optical Lattice (ROL), and it is key for the reconstruction of the trajectories of the signals. The information of the events from IBD is obtained with 75 PMTs connected to three of the faces on the exterior of the detector. The PMTs are in charge of collecting the scintillation light and generating the signals for data extraction. Light is absorbed on a photocathode in a PMT where the energy is transferred to the electrons in the material. These electrons are ejected off from the photocathode as a result of the photoelectric effect and are guided through a series of electrodes in the PMT called *dynodes*[2]. Electrons hit the dynodes and deposit their energy to produce secondary electron emission. These are multiplied and accelerated, due to a difference of voltage between the dynodes, towards an anode that collects them to form electrical signal. The generated signal is then converted into digital signal using an ADC (analog-to-digital converter) for data analysis[1].

### III. CHARACTERIZING A SINGLE CUBE FROM NULAT

#### A. The NaI(Tl) Scintillation Detector

Before we could start collecting any data with NuLat, we had to characterize the response of the detector to eventually calibrate it. At first, we began with a smaller version of the PVT scintillating cubes used in NuLat to thoroughly characterize it. We accomplished this by performing gamma spectroscopy using a thallium-doped sodium iodide (NaI(Tl)) scintillation detector in time coincidence with the single PVT cube. The two parts that mainly compose this detector are the inorganic crystal NaI(Tl) scintillator (from the alkali halide group) and a PMT.

For many years, NaI(Tl) has been the standard scintillation material used due to its popularity in gamma spectroscopy applications. The most prominent feature of NaI(Tl) is its capacity to produce an efficient scintillation light output. The atomic number from one of its constituents, iodine ( $Z=53$ ), contributes to a higher probability for photoelectric absorption to occur in the scintillator which has an impact on the outstanding detection efficiency of NaI(Tl). On the other hand, the thallium is added to act as an activator, whose role is to enhance the scintillation process by increasing the number of photons emitted in the visible range, providing a relatively high light yield. The decay time of the scintillation pulse of NaI(Tl) is 230 ns, making it less suitable at high counting rates, but very effective at low counting rates. Among other significant characteristics of the NaI(Tl) scintillator include its contribution to a larger photofraction (the ratio of the area under the full energy peak to the area under the entire response function) that is independent of the size and shape of the detector[2].

#### B. Coincidence Measurements with Gamma Sources

Taking measurements with two detectors in coincidence is a common technique employed when the goal is to distinguish between the signals from the background and the signals produced by the source. Other applications of radiation detection in coincidence also include the ability to discern different signals that appear in a detector almost simultaneously. In our case, we used this method to characterize a secondary detector using a primary detector with higher resolution by collecting the coincident gamma spectra of different radioactive elements. As mentioned previously, the NaI(Tl) detector was used as our primary detector to thoroughly characterize a single PVT scintillating plastic cube from the NuLat detector. Similar to the NaI(Tl), the PVT detector consisted of the PVT cube scintillator and a PMT. Figure 1 shows both detectors with a gamma source between them before data was taken. Because these two detectors have different sizes and chemical compositions, the NaI(Tl) is expected to project a clearer graph and to collect more events in the higher energy regions than the PVT. The difference in detection efficiency will allow us to understand the response of the PVT using the signals from NaI(Tl). Once the response of the PVT cube is completely determined, we can then extend the information to the full lattice in NuLat.

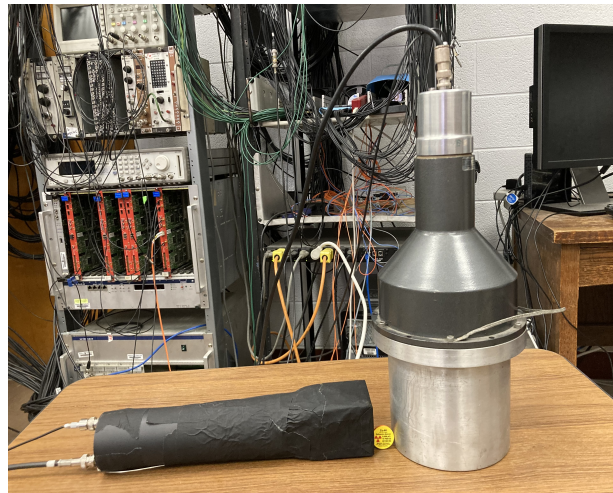


FIG. 1: The PVT detector is shown on the left. It is covered with paper to avoid external light. A sample of Cobalt-60 is in the middle between the PVT and the NaI(Tl) detector shown on the right. The NaI(Tl) scintillator and a PMT are inside the cover of the NaI(Tl) detector.

### 1. Cobalt-60

Our configuration of the experiments consisted of having the two detectors, NaI(Tl) and PVT, next to each other while samples of radioactive sources were placed between them. One of the sources was the radioactive element Cobalt-60, or  $^{60}\text{Co}$ , which served as the gamma emitter.  $^{60}\text{Co}$  decays via  $\beta$  decay emitting an electron ( $\beta^-$  decay) and turning into an excited state of Nickel-60. A gamma ray with energy of 1173 keV is emitted by one of the transitions from the higher energy level to lower energy level states, and almost instantly another gamma ray is emitted with energy of 1333 keV as it reaches the ground state[4]. This process is sketched in an energy level diagram shown in figure 2. When the energy of the gamma ray is fully deposited in the detector, it appears on the gamma spectrum as a full energy peak, or photopeak. For  $^{60}\text{Co}$ , two photopeaks from each of the gamma emissions are expected to be seen on the spectrum. Moreover, because these emissions occur almost simultaneously, their energies can produce a sum peak of the two gammas added together.

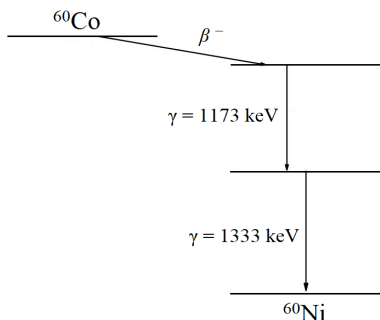


FIG. 2: Energy level diagram of Cobalt-60

### 2. Sodium-22

Another source was Sodium-22 ( $^{22}\text{Na}$ ).  $^{22}\text{Na}$  undergoes  $\beta^+$  decay, meaning that a positron is emitted in the process. A 511 keV peak is expected to appear on the spectrum of  $^{22}\text{Na}$  from the annihilation of the positron with an electron. However, the radiation emitted by pair production results in the emission of two 511 keV gamma rays in opposite directions. If the geometries of the detector allow the absorption of the two pair-produced gamma rays, the full 1022 keV (511 keV + 511 keV) would appear in the spectrum. For our configuration, the two 511 keV could only be collected if they enter both of the detectors at virtually the same time. Instantly  $^{22}\text{Na}$  decays emitting a positron, it turns into the excited state of stable Neon-22, which then goes into ground state where a gamma ray with energy 1275 keV is emitted[4]. Figure 3 shows the beta decay reaction of  $^{22}\text{Na}$ . The gamma spectrum of  $^{22}\text{Na}$  consists of the photopeak from the gamma

and a peak from annihilation radiation. However, it is also possible to observe an extra peak besides these two. The additional peak corresponds to the sum of the aforementioned, which yields an energy value of 1275 keV + 511 keV = 1786 keV.

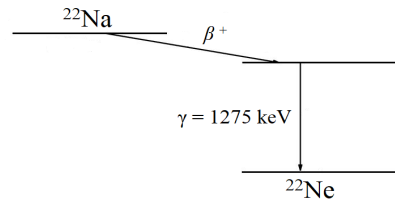


FIG. 3: Energy level diagram of Sodium-22

### 3. Caesium-137

The last gamma source was Caesium-137 ( $^{137}\text{Cs}$ ). This radioactive element is the most preferred for determining an energy calibration due to the less complex interactions of the decay signals with the surroundings.  $^{137}\text{Cs}$   $\beta^-$  decays with the emission of an electron turning into the excited state of Barium-137. A gamma ray of energy 662 keV is emitted as it reaches ground state and will appear as a photopeak in the spectrum when it is fully absorbed. The diagram corresponding to the decay of  $^{137}\text{Cs}$  is also shown in figure 4. The gamma ray does not have enough energy for pair production so annihilation radiation is not expected. Part of the energy in the lower energy range of the spectrum of  $^{137}\text{Cs}$  consists of an x-ray being emitted which will appear as a peak. This occurs when the energy of the gamma is transferred to an electron in the inner shell ejecting it off from the atom, which then is replenished by another electron and in the process a  $K_\alpha$  x-ray takes place[4].

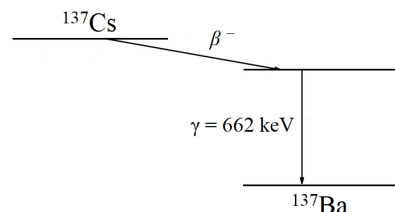


FIG. 4: Energy level diagram of Caesium-137

## IV. RESULTS & CONCLUSIONS

The gamma spectrum of  $^{60}\text{Co}$ ,  $^{22}\text{Na}$ , and  $^{137}\text{Cs}$  are shown in figures 5,6, and 7, respectively. The graphs reflect the expected signals from each of the sources presented above with some additional spectral features of

gamma spectroscopy. These extra features may correspond to *single escape peaks*, *double escape peaks*, *backscatter peaks*, etc. They will appear on the spectrum depending on the source, the size of the detector, and the configuration of the experiment. From the graphs of the gamma spectra obtained with our two detectors in coincidence, the NaI(Tl) demonstrates its greater ability to project the full energy peaks and the inherent signals of gamma detection compared to the PVT detector. The low atomic number  $Z$  of the PVT (a plastic scintillator) influences the probability of photoelectric absorption causing it to mostly detect lower energy depositions. These results allowed us to confirm the responses of the detectors by obtaining the anticipated signals from the radioactive decays plus the possible interactions with the detectors.

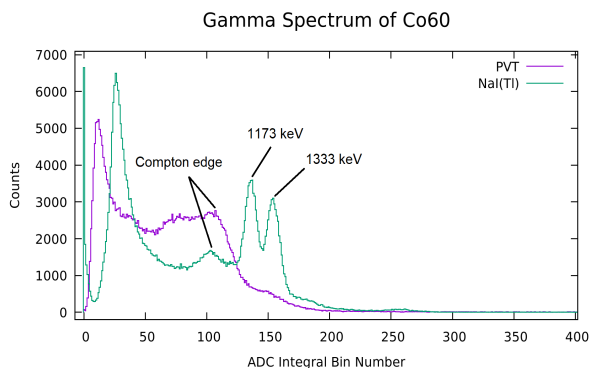


FIG. 5: The gamma spectrum of Cobalt-60 triggered in coincidence between the PVT detector and NaI(Tl) detector.

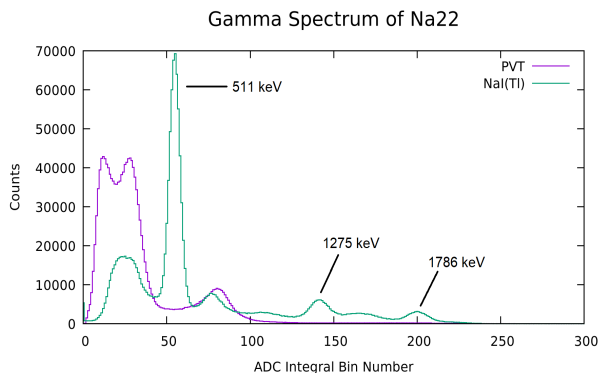


FIG. 6: The gamma spectrum of Sodium-22 triggered in coincidence between the PVT detector and NaI(Tl) detector.

In characterizing the PVT cube, Cobalt-60 was the most effective to analyze the response of the PVT detector due to its two characteristic gamma emissions. They were not only convenient for coincidence triggering but also for studying the coincident spectra of  $^{60}\text{Co}$  taken by the detectors. Because our trigger was set so that signals

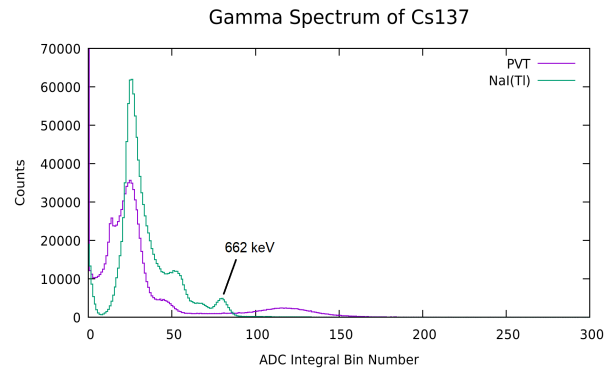


FIG. 7: The gamma spectrum of Caesium-137 triggered in coincidence between the PVT detector and NaI(Tl) detector.

were collected only if they were received in the two detectors, this enabled us to associate the signals of the PVT detector by looking at the response function of NaI(Tl). Therefore, we could infer about either one of the gammas that fully deposited into the PVT from the gamma spectrum obtained with the NaI(Tl) detector.

Figure 5 shows the coincident gamma spectrum of  $^{60}\text{Co}$  with the corresponding signals from the PVT and NaI(Tl). The intrinsic properties of NaI(Tl) are evident from the graph. The two full energy peaks of  $^{60}\text{Co}$  (1173 keV and 1333 keV) appear on the spectrum for NaI(Tl) but are invisible for the PVT. In figure 8, only the spectrum of  $^{60}\text{Co}$  from NaI(Tl) is graphed, where we have performed energy cuts on the photopeaks which are shown in blue and orange in the figure. There are two Compton shoulders (from Compton scattering) that appeared in green and yellow which are associated to the cuts but are hard to see in this graph. In figure 9, the scale of the graph has been changed to log scale to have a better observation on the small number of events. The two Compton shoulders are now visible using this scale and the Compton edge and Compton continuum that correspond to the photopeaks are distinguishable. These are the signals obtained by the PVT detector.

Selecting different cuts on the response function of NaI(Tl) will alter the behavior of the signals of the PVT. The two full energy peaks have been chosen precisely to identify their Compton shoulders. Also, because we can be sure about what the signals that emerge from the cuts are. If we choose to cut on the 1333 keV peak, we would expect to see the signals from Compton scattering of the 1173 keV and vice versa. This is because we can infer that if one of the energies was deposited in one of the detectors, the other must have been deposited at the other detector. Comparing figures 5 and 9, the number of events in the signals of the PVT after performing the cuts have been reduced in figure 9, which means that some of the signal noise has been filtered. In conclusion, this procedure allowed us to clearly identify the signals of the PVT detector from the two gamma rays deposited

in NaI(Tl) and to determine the response of the cube.

The first steps of characterizing a PVT cube from NuLat have been presented in this work. However, further measurements are required to fully characterize the PVT. More testing employing coincidence techniques will be performed and the results will be extended to the full lattice in NuLat. The ultimate goal is to obtain a calibration of the NuLat detector. Along with these experiments, simulations are being processed to compare the experimental results to the expected ones and in this way confirm the efficiency of our method in the characterization of the PVT.

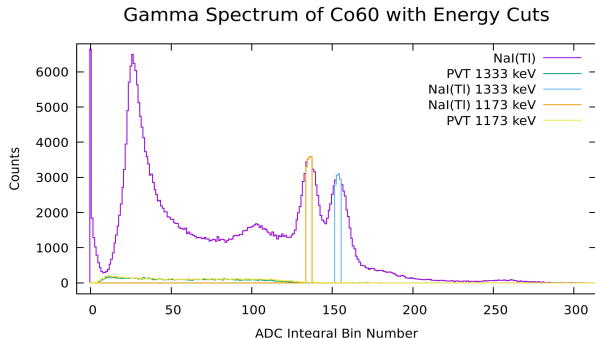


FIG. 8: The gamma spectrum of Cobalt-60 from the NaI(Tl) with energy cuts in **linear scale**.

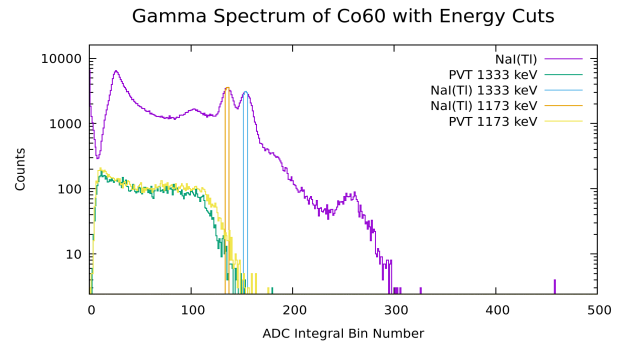


FIG. 9: The gamma spectrum of Cobalt-60 from the NaI(Tl) with energy cuts in **log scale**.

## V. ACKNOWLEDGMENTS

We acknowledge the outstanding support from the National Science Foundation, the Virginia Tech Physics department and the Virginia Tech Center for Neutrino Physics. This work was made possible by the National Science Foundation under grant No. PHY2149165. I would like to thank the immense collaboration and guidance of Tristan Wright and Brian Crow, and the wise mentorship of Dr. Bruce Vogelaar.

- 
- [1] Xinjian Ding. *Development and calibration of NuLat, A new type of neutrino detector*. PhD thesis, Virginia Tech, 2018.
- [2] Glenn F. Knoll. *Radiation Detection and Measurement*. John Wiley & Sons, Inc., Ann Arbor, Michigan, 3rd edition, 1999.

- [3] Kenneth S. Krane. *Modern Physics*. Wiley, New York, 4th edition, 2019.
- [4] L.P. Ekstroem S.Y.F. Chu and R.B. Firestone. *Radioactive sources*, 1999. Last accessed 25 July 2022.